Journal of Materials Chemistry

PAPER

Efficient inverted organic solar cells without an electron selective layer

Jen-Chun Wang,[a] Cheng-Yueh Lu,[c] Jui-Lin Hsu,[b] Ming-Kun Lee,[b] Yun-Ru Hong,[c] Tsong-Pyng Perng,[a] Sheng-Fu Horng*[b] and Hsin-Fei Meng[d]

Inverted organic solar cells which required no electron selective layer were fabricated and their power conversion efficiency was found to improve irreversibly from 1.46% to 4.10% with post-processing light soaking for 2 hours. X-Ray photoelectron spectroscopy characterization revealed further segregation in surface composition at the interface and was found to explain the current density–voltage measurements. In addition, the light soaked devices were found to exhibit extended lifetime as compared to conventional devices. Since no electron selective layer was required, light soaking may be considered as a cost-effective method to achieve efficient inverted organic solar cells.

Introduction

Bulk-heterojunction (BHJ) organic photovoltaic (OPV) devices have attracted considerable attention due to their potential for low-cost manufacturing, mechanical flexibility, light weight and fabrication feasibility.[1–3] One of the most representative BHJ OPV structures is the device based on a blend of poly(3-hexylthiophene) (P3HT) as an electron donor and [6,6]-phenyl C61 butyric acid methyl ester (PCBM) as an electron acceptor.[1,4] In recent years, various new types of donors and acceptors have been synthesized for organic solar cells (OSCs). Many of these devices achieved high power conversion efficiencies (PCEs) and the highest one exceeded 7%.[5,6] This remarkable promotion of cell efficiency has made OSCs more and more promising in commercial applications.

Conventional OSCs generally comprise a low work function cathode which oxidizes easily in air. Therefore, these devices exhibit poor air stability.[7] In addition, it has been reported that the vertical distribution of donors and acceptors in BHJ OSC exhibits higher concentration of acceptor at the ITO side.[8] Such a vertical concentration gradient of donor and acceptor is unfavorable for charge transport in conventional OSCs. One way to overcome this drawback is to use the inverted structure which exploits the vertical concentration distribution and employs only stable electrode materials with high work function. Previously, materials such as cesium carbonates (Cs_2CO_3),[9] titanium dioxide (TiO_2)[10] and zinc oxide (ZnO)[11–13] thin films have been used as electron selective layers to improve the electron transport ability

in inverted OPV devices. In our previous study, we prepared the ZnO electron selective layer by atomic layer deposition (ALD) for inverted OPV devices on flexible substrates and achieved a PCE of 4.18%.[14] So far, it seems that electron selective layer is necessary in inverted OPV devices to achieve high efficiency. However, the preparation of electron selective layer usually requires sophisticated processing step such as ALD or poses new problems on uniformity control such as nanoparticle coating. Although significant progress has been made recently in enabling processing of Al-doped ZnO using roll-to-roll methods from solvents such as methanol and water,[15,16] the possibility to spare oneself from the fabrication of electron-selective layer may be attractive and help simplify the processing of inverted organic solar cells.

Herein, we report an efficient inverted OPV device in which an electron selective layer is not used. We found that a post-processing continuous illumination on an ITO/P3HT:PCBM/ PEDOT:PSS/Ag device enhanced the PCE from 1.46% to 4.10%. X-Ray photoelectron spectroscopy (XPS) was employed to study the surface composition of blend layers and the results were correlated to the current density–voltage (J–V) measurement.

Experimental

Device fabrication

The schematics of our device structure and band diagram are shown in Fig. 1. To fabricate the device, indium tin oxide (ITO)-coated glass substrates were first cleaned in an ultrasonic bath with acetone, isopropanol and de-ionized water for 10 min, respectively. A blend solution of P3HT (17 mg ml^{-1}, purchased from Rieke Metals) and PCBM (17 mg ml^{-1}, purchased from Nano-C) was prepared using 1,2-dichlorobenzene (DCB) as a solvent and stirred vigorously over 12 hours. The blend solution was then spun onto the ITO-coated substrate at 600 rpm in a glove box, followed by the spin coating of a PEDOT:PSS (P VP

[a]Department of Materials Science and Engineering, National Tsing Hua University, Hsinchu, 30013, Taiwan
[b]Institute of Electronics Engineering, National Tsing Hua University, Hsinchu, 30013, Taiwan. E-mail: sfhorng@ee.nthu.edu.tw
[c]Institute of Photonics Technologies, National Tsing Hua University, Hsinchu, 30013, Taiwan
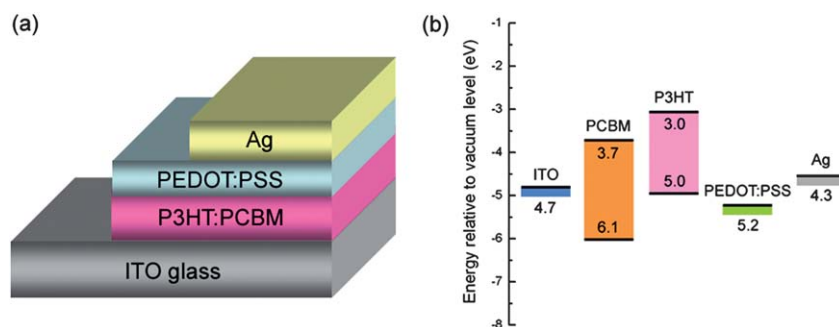*[d]Institute of Physics, National Chiao Tung University, Hsinchu, 30013, Taiwan*

Fig. 1 (a) The device structure and (b) the energy band diagram of the inverted organic solar cell investigated in the present study.

AI 4083, purchased from H. C. Starck) solution diluted in isopropanol (IPA) with a weight ratio of 1 : 5 (PEDOT:PSS : IPA). Both of the blend and PEDOT:PSS layer were annealed at 140 °C for 10 min, respectively. Subsequently, the devices were completed with the deposition of an 80 nm thick Ag top electrode by thermal evaporation. The area of device is 4 mm^2.

Device characterization

The J–V characteristics of the devices were measured with a Keithley 2400 source measurement unit using a 100 mW cm^{-2} AM 1.5G solar simulator (San-ei Electric, XES-301S). The intensity of the incident solar illumination was calibrated by a silicon photodiode (HAMAMATSU S1337-BR). The same solar simulator was used for post-processing continuous illumination. The external quantum efficiency (EQE) was conducted using a measurement system (model QE-R) built by Enli Technology Co. Ltd. Wide-spectrum light source is chopped and diffracted into separated monochromatic narrow bands, and each of which is projected onto the device under testing. The photo-current generated by incident monochromatic light is converted and amplified to an AC voltage by a trans-impedance amplifier, which is then measured by a lock-in amplifier at the chopper frequency. Surface roughness and morphology of the blend films were observed by atomic force microscopy (AFM, model: Dimension 3100, Veeco). The XPS (Thermo Microlab 350) measurements were conducted inside an ultrahigh vacuum system. The XPS spectra were measured utilizing Mg Kα (1253.6 eV) X-ray source for the surface composition of the blend layers.

Results and discussion

Fig. 2 shows the J–V curve of the devices before (as prepared) and after continuous illumination (light soaking) under an AM 1.5G solar simulator for 2 hours. Unlike conventional diode-like behavior, the dark J–V curve of the as-prepared device exhibits leakage at negative bias and was suppressed at forward bias. The illuminated J–V curve of the as-prepared device shows similar leakage at negative bias and rises quickly around $V = 0$ V, leading to a small open-circuit voltage (V_{oc}) of 0.36 V. It is also notable that the current density is also suppressed at forward bias, resulting in an inflection point near V_{oc}. As a result, the as-prepared device yields small fill factor (FF) and poor PCE. For the devices with light soaking, not only the current leakage at the negative bias but the inflection near the V_{oc} disappears in the

illuminated J–V curve, exhibiting normal diode-like characteristics. This disappearance of inflection with light soaking is similar to observation previously reported from inverted organic solar cells with ZnO electron-selective layer.[17] In our cases, the V_{oc} (FF) increases from 0.36 V (0.40) for the as-prepared device to 0.62 V (0.57) for the devices with light soaking. Because both V_{oc} and FF are significantly enhanced after light soaking, the PCE is also greatly enhanced from 1.46% to 4.10%. The photovoltaic parameters are summarized in Table 1.

Fig. 3(a) and (b) show the absorption of the blend layer coated on ITO substrates and the EQE of the inverted devices, with or without light soaking, respectively. It can be seen from Fig. 3(a) that the absorption of blend layer does not change with light soaking. However, the EQE spectrum of light-soaked device is higher than that of the as-prepared device. This indicates that the light-soaked device has better carrier transport and carrier collection efficiency.
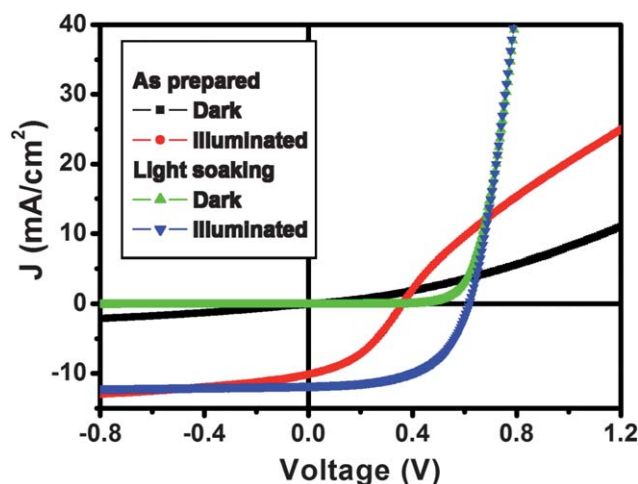

Fig. 2 The J–V characteristics of the as-prepared and light-soaked inverted organic solar cells in the dark and under illumination.

Table 1 Summary of the performance parameters of the as-prepared and light-soaked inverted organic solar cells

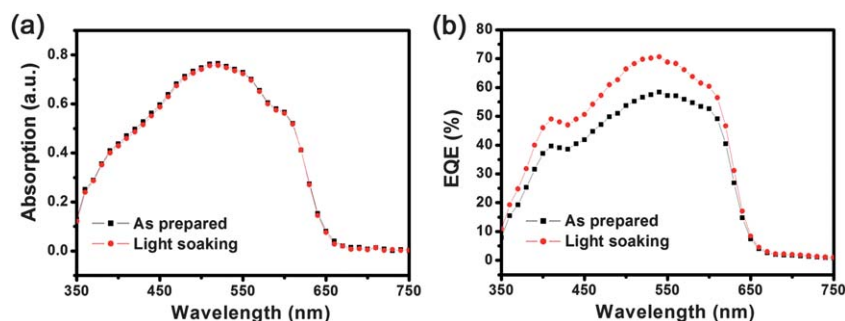|	J_{sc} mA cm^{-2}	V_{oc}/V	FF	PCE (%)
As prepared	10.14	0.36	0.40	1.46
Light soaking	11.73	0.62	0.57	4.10

Fig. 3 (a) The absorption and (b) the EQE spectra of the as-prepared and light-soaked inverted organic solar cells, respectively.

To investigate whether the aforementioned light-soaking induced enhancement is due to the increase in substrate temperature, which is measured to be around 50 °C, the effect of post-annealing was studied. Fig. 4(a) and (b) show the illuminated J–V curves of devices which were post-annealed at 50 °C and 60 °C, respectively, and the performance parameters are summarized in Table 2. Though the leakage current at reverse

Fig. 4 The J–V characteristics of the inverted organic solar cells post-annealed at (a) 50 °C and (b) 60 °C, respectively.

Table 2 Summary of the performance parameters of the as-prepared and post-annealed inverted organic solar cells

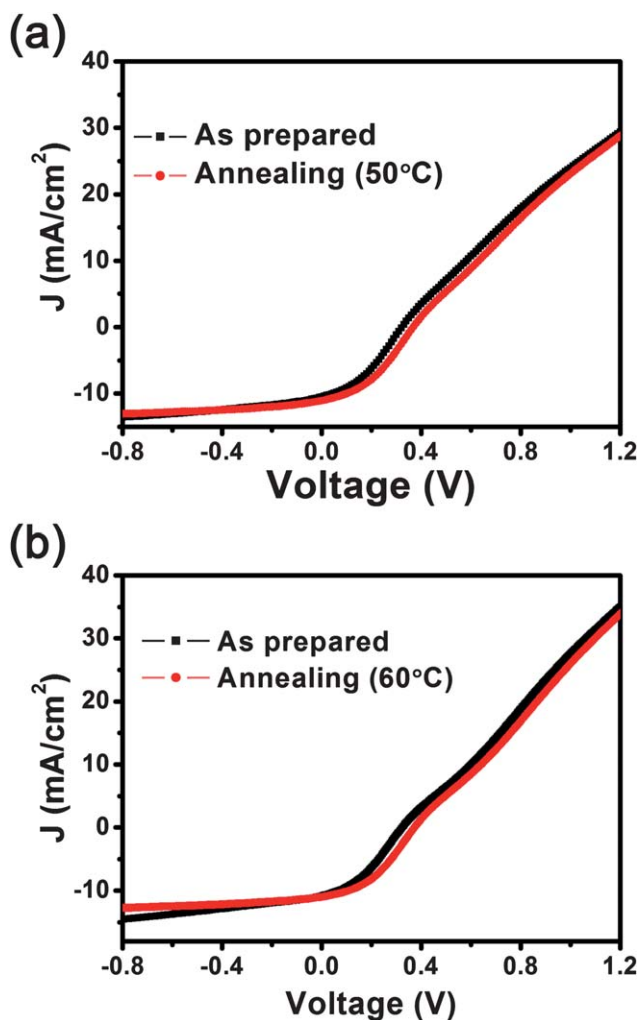|	J_{sc} mA cm^{-2}	V_{oc}/V	FF	PCE (%)
Device A				
As prepared	10.48	0.32	0.37	1.26
Annealing (50 °C)	11.07	0.37	0.39	1.59
Device B				
As prepared	10.85	0.32	0.37	1.30
Annealing (60 °C)	10.99	0.37	0.41	1.66

bias was reduced, the J_{sc}, V_{oc}, FF and thus PCE of both devices with post-annealing remain nearly unchanged. Hence, the light-soaking induced enhancement was not attributed to the increase in substrate temperature during the illumination.

In order to understand the effects of post-treatments, XPS was employed to characterize the surface composition of blend layers. The samples for XPS characterization were prepared in the same way as described previously except that they were not coated with PEDOT:PSS and metal electrode. These samples were then encapsulated with glass and subject to different post-treatments. Three types of samples were compared: (A) as prepared, (B) post-annealed at 50 °C for 2 hours and (C) light soaked for 2 hours. The glass covers of the samples were detached immediately before loading into the XPS chamber. Sulfur (S) 2p and carbon (C) 1s signals were detected. Thermo Avantage software (v3.20) was used to calculate the S to C atomic ratios, which in turn were transformed to P3HT to PCBM relative weight percentage. The measured S 2p core levels were shown in Fig. 5 and the calculated results were summarized in Table 3. It is clear from Fig. 5 that the as-prepared sample and post-annealed sample exhibited similar sulfur (S) 2p intensities which were obviously lower than that of the sample with light soaking. While the P3HT weight ratio of as-prepared sample and post-annealed sample is around 60%, it was increased to 75% for the light-soaked sample. Accordingly, P3HT was further segregated at the surface of the blend layer after light soaking.

It is noteworthy to mention that XPS provides only the surface concentration within the electron escape depth and techniques such as Time-of-Flight Secondary Ion Mass Spectrometry (TOF-SIMS) depth profiling, XPS depth profiling and ellipsometry should be used to provide more detailed information on vertical concentration profile, which are essential to understand the microscopic mechanism and to devise post-processing with
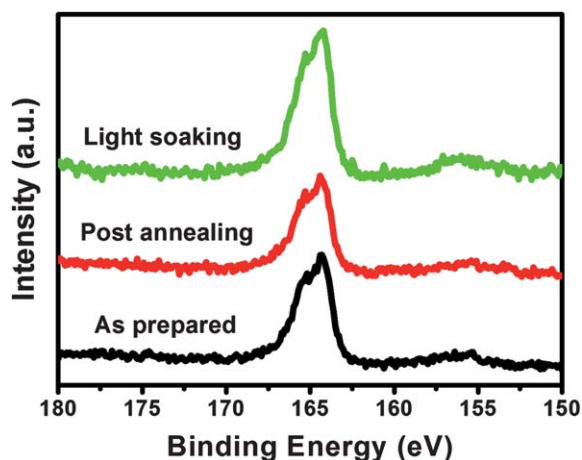
This journal is © The Royal Society of Chemistry 2011

J. Mater. Chem., 2011, **21**, 5723–5728 | 5725

Fig. 5 The XPS spectra of S 2p obtained from the surface of P3HT/PCBM blend layers with different post-treatments.

reduced time. Nevertheless, we found that a tentative explanation of the J–V curves based on the vertical segregation of P3HT can be made as follows.

To help understanding the effects of light soaking on the J–V curves, the schematics of band diagrams for our inverted devices at various biases were shown in Fig. 6. As shown in Fig. 6(a), since ITO has a larger work function than silver, the built-in potential disfavors electron (hole) transport to ITO (Ag) electrode at $V = 0$ V. Besides, it was reported that PEDOT:PSS is not an effective electron blocking layer.[18] Photo-carriers might travel toward wrong electrode and recombine among themselves due to their more uniform distribution within the devices.[19] Consequently, the early rise of current density around $V = 0$ V

Table 3 Atomic and weight ratios of the surface composition in P3HT/PCBM blend layers subject to different post-treatments

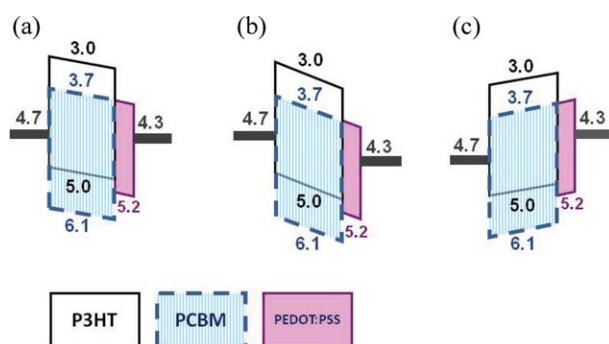|	Atom (%)		Weight (%)	
	C 1s	S 2p	PCBM	P3HT
As prepared	94.93	5.07	40.1	59.9
Post-annealing	94.77	5.23	38.3	61.7
Light soaking	93.44	6.56	24.5	75.5

Fig. 6 The schematics of band diagrams for the inverted organic solar cells at (a) $V = 0$ V, (b) forward bias and (c) reverse bias.

for the as-prepared sample, as observed in Fig. 2, was expected. With light soaking for 2 hours, there is much more P3HT segregating at the interface between the blend layer and PEDOT:PSS. The segregated P3HT layer would efficiently block the electrons transport from PCBM to the Ag anode, leading to blocked electrons accumulated at the interface. The accumulation of electrons at the blend/PEDOT:PSS interface decreases the bulk electric field and enhances the electron diffusion to the ITO cathode. The rise of the current density observed at $V = 0$ from the as prepared sample is therefore retarded, leading to increased V_{oc}.

It is to note that since the energy barrier against electron injection from electrodes into the device is much larger than that against hole injection, the electron injection in our devices is negligible at all biases. It is also noteworthy from Fig. 6(b) that the forward current results dominantly from the collection of photo-carriers as well as the injection of holes from the Ag anode. The inflection of J–V curves around V_{oc} for the as-prepared device indicates that the hole injection from the anode[20] is limited and the current comprises mostly the photo-carriers, leading to suppressed current at forward bias (Fig. 2). On the other hand, the suppression of hole injection in the light-soaked device is lifted and the forward current exhibits normal diode-like. In view of the P3HT surface segregation induced by light soaking, we attributed tentatively the suppression of hole injection to the limited P3HT surface concentration. It is remarkable that a mere increase in the P3HT surface composition ratio from 59% to 75% eliminates the current suppression and restores the diode-like J–V characteristics.

From the band diagram shown in Fig. 6(c), the leakage at reverse bias for the as-prepared devices should result dominantly from the hole injection from ITO into the active layer. The observation of diminished leakage current at reverse bias in the case of light-soaked device also suggests that the relative amount of PCBM at the ITO/blend interface increases after light soaking, thus inhibiting the hole injection from ITO to the blend.

AFM was used to understand whether the light-soaking process would induce the change in film morphology. Fig. 7(a) and (b) display the AFM images of the blend surface of the as-prepared and light-soaked sample, respectively. Larger aggregation is observed on the blend surface of the light-soaked sample than the as-prepared sample. The surface roughness increases from 3.9 nm to 6.9 nm with light soaking. The results indicate that significant mass transport takes place although the detailed microscopic mechanism is unclear and requires further study. Li *et al.* suggested that rough surface morphology may reduce the charge-transport distance and increase the J_{sc}.[21] The increase in J_{sc} from 10.1 to 11.7 mA cm^{-2} is therefore attributed to the rougher surface morphology induced by light soaking.

The photovoltaic parameters of the light-soaked devices were measured to check if the light-soaking induced enhancement is reversible. The device was kept in a glove box for the first 16 days and was moved to air ambient thereafter. Fig. 8 shows the evolution of the performance parameters as a function of storage time. Day 0 denotes the day on which the device was prepared and light soaked. Although J_{sc} slightly decreased, V_{oc} and FF remained relatively constant and the PCE of the device maintains more than 90% over the entire time duration. It was also observed that the PCE, V_{oc} and FF increased slightly when the
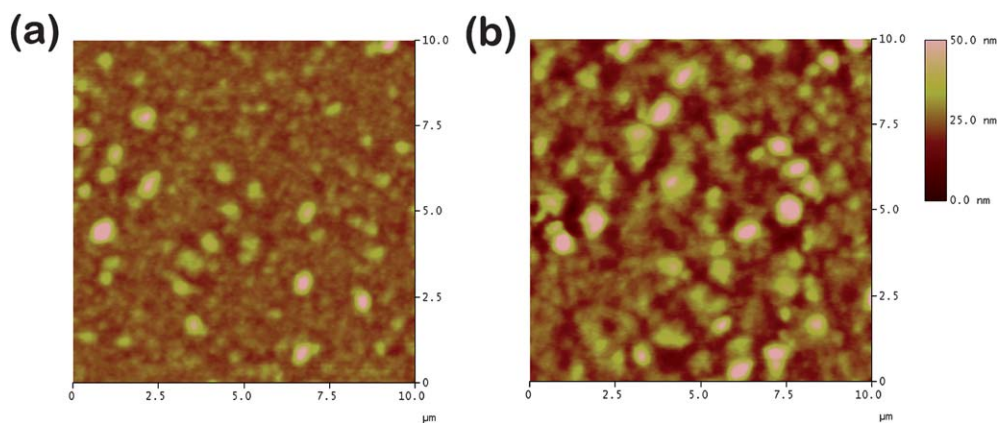
5726 | *J. Mater. Chem.*, 2011, **21**, 5723–5728

This journal is © The Royal Society of Chemistry 2011

Fig. 7 AFM images of the (a) as-prepared and (b) light-soaked P3HT/PCBM blend layer surface morphology.
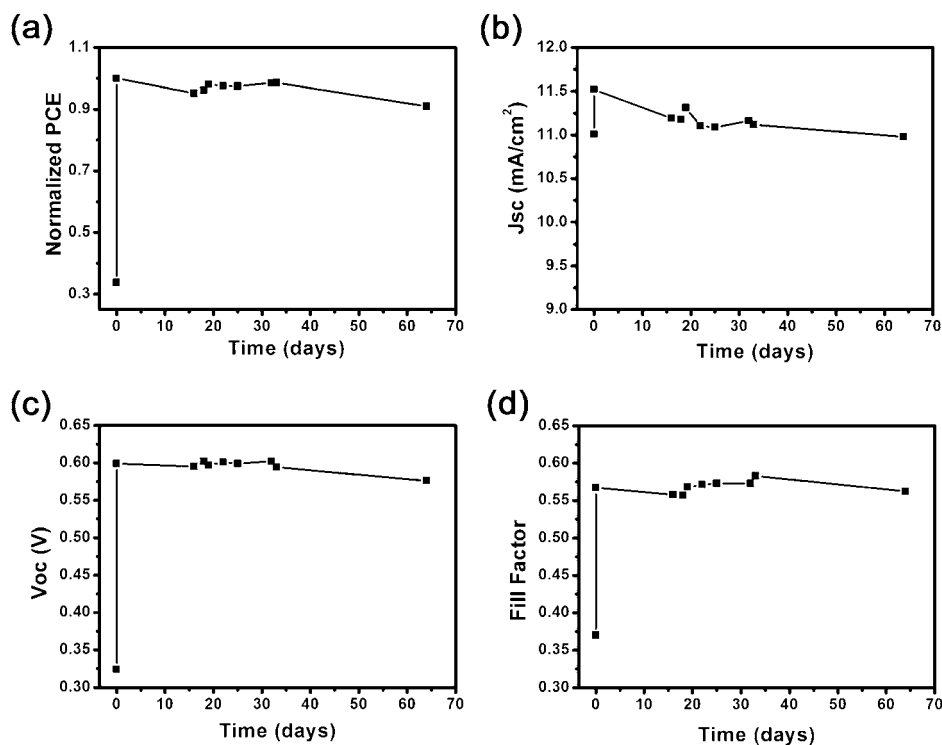

Fig. 8 The evolution of the performance parameters as a function of storage time: (a) PCE, (b) J_{sc}, (c) V_{oc} and (d) FF.

device was moved to air ambient. The slight improvement may result from the oxidation of silver electrode, which was reported to increase the Ag work function.[22] With larger Ag work function, the built-in potential would favor more the charge transport to the electrode in inverted OPV device. It is clear from this result that the light-soaked device shows good air stability and the light-induced enhancement is irreversible, as compared to reversible enhancement reported in the literatures.[23,24]

Conclusions

In summary, inverted organic solar cells without electron selective layer were fabricated and a post-processing light soaking for two hours with an AM 1.5G solar simulator was found to improve the PCE from 1.46% to 4.10% irreversibly. The improvement in photovoltaic response was tentatively attributed to the change in surface composition of blend layers, which is more favorable for charge transport in inverted structures. Further investigation by TOF-SIMS depth profiling, XPS depth profiling and ellipsometry is required to understand the microscopic mechanism of light-induced enhancement. Since the light-induced enhancement is irreversible, light soaking may be used as a new cost-effective method to achieve efficient inverted OPV devices.

Acknowledgements

References

1 B. C. Thompson and J. M. J. Fréchet, *Angew. Chem., Int. Ed.*, 2008, **47**, 58.
2 F. C. Krebs, *Sol. Energy Mater. Sol. Cells*, 2009, **93**, 394.
3 C. N. Hoth, S. A. Choulis, P. Schilinsky and C. J. Brabec, *J. Mater. Chem.*, 2009, **19**, 5398.
4 H. Hoppe and N. S. Sariciftci, *J. Mater. Chem.*, 2006, **16**, 45.
5 Y. Liang, Z. Xu, J. Xia, S. T. Tsai, Y. Wu, G. Li, C. Ray and L. Yu, *Adv. Mater.*, 2010, **22**, 1.
6 G. Zhao, Y. He and Y. Li, *Adv. Mater.*, 2010, **22**, 4355.
7 J. Huang, G. Li and Y. Yang, *Adv. Mater.*, 2008, **20**, 415.
8 Z. Xu, L. M. Chen, G. Yang, C. H. Huang, J. Hou, Y. Wu, G. Li, C. S. Hsu and Y. Yang, *Adv. Funct. Mater.*, 2009, **19**, 1.
9 H. H. Liao, L. M. Chen, Z. Xu, G. Li and Y. Yang, *Appl. Phys. Lett.*, 2008, **92**, 173303.
10 C. Tao, S. Ruan, X. Zhang, G. Xie, L. Shen, X. Kong, W. Dong, C. Liu and W. Chen, *Appl. Phys. Lett.*, 2008, **93**, 193307.
11 F. C. Krebs, *Org. Electron.*, 2009, **10**, 761.
12 F. C. Krebs, *Sol. Energy Mater. Sol. Cells*, 2008, **92**, 715.
13 S. K. Hau, H. L. Yip, N. S. Baek, J. Zou, K. O'Malley and A. K. Y. Jen, *Appl. Phys. Lett.*, 2008, **92**, 253301.
14 J. C. Wang, W. T. Weng, M. Y. Tsai, M. K. Lee, S. F. Horng, T. P. Perng, C. C. Kei, C. C. Yu and H. F. Meng, *J. Mater. Chem.*, 2010, **20**, 862.
15 R. Søndergaard, M. Helgesen, M. Jørgensen and F. C. Krebs, *Adv. Energy Mater.*, 2011, **1**, 68.
16 J. Alstrup, M. Jørgensen, A. J. Medford and F. C. Krebs, *ACS Appl. Mater. Interfaces*, 2010, **2**, 2819.
17 M. R. Lilliedal, A. J. Medford, M. V. Madsen, K. Norrman and F. C. Krebs, *Sol. Energy Mater. Sol. Cells*, 2010, **94**, 2018.
18 A. L. Ayzner, D. D. Wanger, C. J. Tassone, S. H. Tolbert and B. J. Schwartz, *J. Phys. Chem. C*, 2008, **112**, 18711.
19 Y. X. Wang, S. R. Tseng, H. F. Meng, K. C. Lee, C. H. Liu and S. F. Horng, *Appl. Phys. Lett.*, 2008, **93**, 133501.
20 A. Kumar, S. Sista and Y. Yang, *J. Appl. Phys.*, 2009, **105**, 094512.
21 G. Li, V. Shrotriya, J. Huang, Y. Yao, T. Moriarty, K. Emery and Y. Yang, *Nat. Mater.*, 2005, **4**, 864.
22 M. T. Lloyd, D. C. Olson, P. Lu, E. Fang, D. L. Moore, M. S. White, M. O. Reese, D. S. Ginley and J. W. P. Hsu, *J. Mater. Chem.*, 2009, **19**, 7638.
23 Y. Zhou, H. Cheun, W. J. Potscavage, Jr, C. Fuentes-Hernandez, S. J. Kim and B. Kippelen, *J. Mater. Chem.*, 2010, **20**, 6189.
24 H. Schmidt, K. Zilberberg, S. Schmale, H. Flügge, T. Riedl and W. Kowalsky, *Appl. Phys. Lett.*, 2010, **96**, 243305.